

Improved Reactive Power Management Strategy for Photovoltaic Based Distributed Generators

Neha Shah^{*‡}, Urvi Patel^{**}, Hiren Patel ^{***}

* Department of Electrical Engineering, Sardar Vallabhbhai Patel Institute of Engineering, Vasad, Anand, Gujarat, India.

** Department of Electrical Engineering, Dr. S. & S. S. Ghandhy Government Engineering College, Majura Gate, Surat, Gujarat, India.

*** Department of Electrical Engineering, Sarvajanic College of Engineering and Technology, Athwalines, Surat, Gujarat, India.

(neha_saurabh_shah@yahoo.com, urvip3004@gmail.com, hiren.patel@scet.ac.in)

[‡]Corresponding Author; Neha Shah, Department of Electrical Engineering, Sardar Vallabhbhai Patel Institute of Engineering, Vasad, Anand, Gujarat, India, neha_saurabh_shah@yahoo.com

Received: 06.08.2018 Accepted:30.09.2018

Abstract- Reactive power sharing amongst photovoltaic based distributed generators (DGs) operating in parallel is a challenging task. As the active power supplied by these DGs depend on environmental conditions, reactive power margin (the maximum reactive power that DG can supply) varies. Hence, the reactive power supplied by these DGs must be varied accordingly, to avoid unequal utilization and/or overloading of the DGs. Few reactive power sharing algorithms have tried to target this issue. However, they do not ensure equal percentage utilization of the DGs. Further hardly any of these algorithms have focused on the efficiency of the system in relation to apparent power shared by the inverters. The proposed reactive power sharing algorithm, referred as equal apparent power sharing with least losses (EAPS-LL), focuses on these two objectives. It assigns the reactive power amongst the DGs based on the reactive power margins of the DGs. Hence, it ensures nearly equal utilization of inverters thereby avoiding overloading of the inverters. The algorithm also evaluates various possible sequences in which reactive power allocation can be carried out and identifies the sequence that results into the least losses. The effectiveness of the proposed algorithm over other algorithms is highlighted through results obtained in MATLAB/Simulink.

Keywords photovoltaic, power sharing, reactive power, ORPS, EAPS, EAPS-LSD.

1. Introduction

Photovoltaic (PV) based distributed energy generation has gained a lot of popularity in the last couple of decades due to one or more of the following features: ease of commissioning, less gestation period, modularity, possibility to introduce it into the system at distribution level, freeing up of transmission capability, lesser line losses, generation from clean source, etc. [1]. However, the efficiency of the PV cell is quite low and hence, requires large number of modules to generate the power in the range of MW. It demands large space and extra investment for the frame/structure for installation of modules. Hence, it is advisable to extract as much power as possible from the PV array to make the overall system as efficient and as small as possible.

Extracting the maximum power from the PV array under uniform conditions (similar irradiance, temperature and environmental conditions for all modules) is not that difficult. The output power under such conditions is not affected by the array configurations like series-parallel, total-cross-tied, bridge-linked etc [2]. Further it is easy to extract the maximum power from the PV array using conventional maximum power point tracking (MPPT) techniques like perturb-and-observe or incremental conductance[3-5]. However, under partially shaded conditions these techniques fail as they are unable to differentiate between the global peak and the local peaks present on the $P-V$ characteristics of the array. Several global peak power point tracking techniques based on principle of scanning the characteristic, artificial intelligence, and evolutionary algorithms like

particle swarm optimization, genetic algorithm, ant-bee colony etc. have been reported to track the global peak [6-9]. The effect of partial shading can also be minimized by allowing the reconfiguration of the arrays [10] or by applying the concept of distributed maximum power point tracking (DMPPT). In DMPPT approach, a power electronic dc-dc converter is attached with each module, thereby allowing one to track the peak of the $P-V$ characteristic of each module [11-12]. Thus, rather than operating on the resultant $P-V$ characteristic of the PV array, it is ensured that each converter operates independently on the $P-V$ characteristic of the associated module. Hence, maximum possible power can be extracted. Both these approaches, reconfiguration and DMPPT, suffers from the disadvantage of higher cost due to higher number of sensors and switches. Some researchers have even focused on other avenues of minimizing the losses. In [13], the optimal power flow (OPF) is considered for microgrids (MG), with the objective of minimizing the power distribution losses, power electronics converter losses and the cost of power drawn from the DG units. A multi-objective optimization problem that investigates the OPF problem for distribution networks with the integration of DG is proposed in [14]. In addition to the DG's active-power output, criteria like line loss and voltage deviation are considered in the objective function. Genetic algorithm-based OPF [15] also focuses on minimizing the losses in power electronic converters and dc distribution lines for optimal dc voltage and power control in autonomous MGs. Thus, considerable efforts have been made by the researchers over the years to improve the efficiency of the overall PV system by targeting different aspects of the PV system.

Earlier most of the grid-connected DGs were allowed to supply only active power into the grid and were not allowed to play role in voltage and frequency control. Hence, the major focus was on active power control and improving the efficiency of the system. But recently policies have been relaxed by the regulator bodies whereby the DGs are now allowed to even exchange the reactive power with the grid to have participation in voltage control [16]. So many researchers have now focussed on the issues related to the reactive power management amongst the DGs operating in the microgrid. However, the reactive power management; especially when several PV based DGs are connected in parallel or operating in a grid is a challenging task [17].

The most popular approach for power management or active and reactive power sharing amongst the DGs operating in the MG is the droop control technique [18-19]. The conventional droop control technique does not require any communication channel between DGs and employs active power versus frequency ($P-\omega$) and reactive power versus voltage ($Q-V$) droop to share active and reactive power amongst the DGs. But the conventional $P-\omega$ droop technique is characterized by fixed droop coefficient [20]. In such case, if the output power of one of the PV based DG decreases, the frequency increases. As other DGs must operate at the same frequency, they must reduce their output, thereby forcing the auxiliary source to supply more power. Further, as the active power that the PV based DG can supply vary, the available margin for the DG to support the reactive power also varies. Thus, the reactive power injection/absorption capability is

actually constrained by the available margin with the inverter besides that of the local load requirement and/or the grid regulations [21]. However, fixed $Q-V$ droop based control ignores it and hence, if the reactive power demand increases, it is shared amongst the inverters as per the fixed droop set initially. As a result, the inverter of the DG supplying more active power is likely to operate near its rating or may get overloaded [21].

Reactive power can also be shared simply by assigning equal reactive power reference to each DG as done in equal reactive power sharing [ERPS] algorithm based droop control method [22]. It shares reactive power demand equally amongst the inverters irrespective of variation in active power. Hence, it results into unequal utilization of inverters. A two-layer distributed average control scheme employing a multi-agent system [23] also focuses on voltage and reactive power control amongst the DGs operating in a microgrid. It avoids the need of central controller and involves a sparse communication between the DGs to achieve accurate reactive power control. However, it also shares the reactive power equally amongst the DGs and nothing has been mentioned about the variation in the reactive power vis-à-vis the variations in the active power.

Another approach, known as quasi-master-slave control approach [24], with adaptive droop-settings for active and reactive power control can take care of the varying environmental conditions and distributes the reactive power more uniformly amongst the DGs. This helps in minimizing the difference in the percentage utilization of the inverters. The adaptive droop control which enables the maximum utilization of the volt-ampere (VA) rating of the inverter in a PV/battery hybrid system is also reported in [25]. It also adjusts the reactive power references (or droop settings) for the inverter as per the variation in the active power of PV based DG. However, as the references are set locally without any secondary control involving communication with other DGs, overall system losses may increase.

Various other control approaches that can be employed as a secondary control to provide the reactive power references for the droop control are presented in [26-28] to share reactive power amongst PV based DGs operating in parallel. Optimum reactive power sharing algorithm (ORPS) reported in [26], which aims to maximize the cumulative reactive power capability of the inverters, shares the reactive power amongst the inverters in proportion to the active power supplied through the inverters. It optimizes the reactive power capability of the inverters, but at the cost of unequal utilization of the inverters under partially shaded conditions. Some of the inverters may operate near its full capacity while some may be least utilized. This results into unequal heating of the similar components of different inverters. Further, it may not result into the best possible solution in terms of the lower losses in the inverters. Unlike it, the equal apparent power sharing (EAPS) algorithm [29] ensures that the reactive power is assigned to the inverters such that apparent power capability of each inverter is equally utilized. The EAPS algorithm assigns reactive power to each inverter in terms of the available margin of the inverter. The modified EAPS i.e. equal apparent power

sharing with least standard deviation (EAPS-LSD) [30], focuses on the order in which the reactive power is assigned to the inverter and identifies the solution that gives the least standard deviation of the utilization factors of the inverters. In EAPS-LSD while achieving the equal apparent power sharing, the total power loss (summation of power loss in the inverters and their interfaces) may increase. Thus, EAPS and EAPS-LSD approaches emphasize on just equalizing the utilization of the inverter and do not focus on the increase in the power losses in the inverters that occurs during realizing the objective of equal utilization of the inverters.

The paper presents a modified algorithm that takes both these important aspects (equal utilization and minimization of losses) into account to have the effective and efficient utilization of the PV system. This algorithm referred as 'equal apparent power sharing with least loss' (EAPS-LL) shares the reactive power in such a way that not only the apparent power is shared equally amongst the inverters, but also ensures that the objective is achieved with the least possible losses. Section-2 describes MG system having 'm' identical grid connected PV based DGs and the control scheme for the inverters. The detailed EAPS-LL algorithm is incorporated in section-3. The results with the proposed algorithm for different cases are discussed in section-4 which is followed by the conclusion in section-5.

2. System Description and Control

Figure 1 shows the MG system comprising of 'm' number of PV based DGs connected to the main grid through a three-phase inverter. The DGs are connected to the point of common coupling (PCC) through a transformer which is not shown in Fig. 1 for the sake of simplicity. Z_{oi} , where 'i' represents i^{th} DG, is the total impedance of interfacing inductor, cable and transformer. PV_i in the Fig. 1 represents i^{th} PV array and a boost converter where boost converter not only helps in stepping up the voltage but also extracts the maximum power from the PV array.

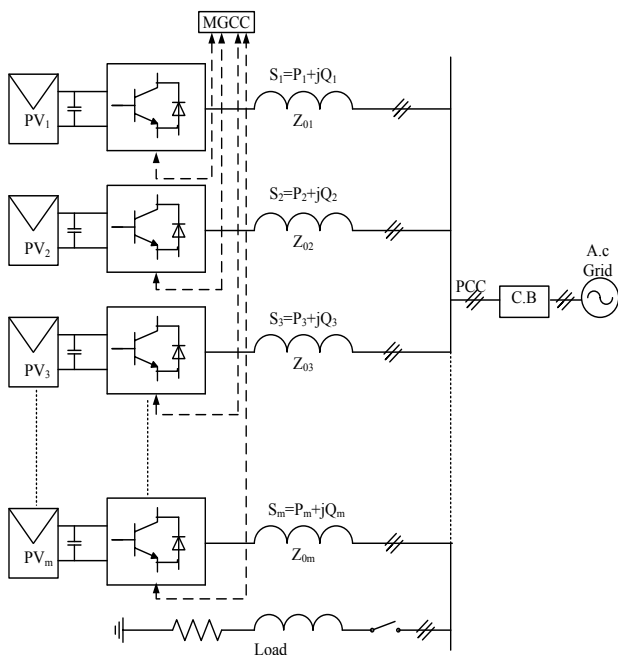


Fig. 1. System configuration of a Microgrid with 'm' DGs.

Inverter control is achieved by active-reactive power control method so that the desired active and reactive power can be exchanged with the grid by controlling the inverter as a controlled current source. It employs two loops one inner current control loop to regulate inverter output current and another outer power loop for intended power exchange. The power control loop sets the reference for inner current loop while the active and reactive power references for the power control loop is obtained from the MPPT algorithm and the proposed algorithm (discussed in next section), respectively. Additionally, a voltage control loop is required to ensure a tight voltage regulation at the DC bus. The control scheme is presented in detail in [29].

3. Reactive Power Sharing Algorithm

The control principle employed is based on the fact that the apparent powers of the inverters can be made equal if the DG that generates lesser active power must supply more reactive power and vice-versa. The principle is highlighted through Fig. 2 showing power sharing among four identical DGs are considered.

As shown in Fig. 2, the total apparent power requirement $S_T = P_T + jQ_L$ can be met if all the DGs supply apparent power $S_T/4$ at the same power factor. Here, $P_T = \sum_{i=1}^4 P_i$ represents the total active power generated by the DGs and $Q_L = \sum_{i=1}^4 Q_i$ is the reactive power demand of the load, while P_i and Q_i are the active power and reactive power supplied by i^{th} DG, respectively, where $i=1$ through 4. Thus, if all the DGs supply apparent power $S_T/4$ at the same power factor, $P_1 = P_2 = P_3 = P_4$ and reactive power $Q_1 = Q_2 = Q_3 = Q_4$ for inverters $i=1$ through 4. In this case utilization of inverters of the DGs (in terms of the ratio of the apparent power supplied to the nominal rating of the inverter) for all the DGs is the same. However, as the active power of the PV based DGs is dependent on environmental conditions (like irradiance, temperature, shading due to clouds etc.), active power generated by all these DGs may be different. Hence, their reactive powers must be adjusted such that magnitudes of the apparent power (S_i) of these inverters are equal. This is represented in fig. 2 by the vectors S_1 through S_4 of equal length (shown with black lines). The principle of determining S_i to achieve the equal magnitudes of the apparent power supplied by DGs is explained next.

The PV based DGs generating active powers P_1 through P_4 , are operated such that they must try to meet the total reactive power demand Q_L of the load. Hence, the total apparent power to be handled by the inverters is

$$S_T = \sqrt{P_T^2 + Q_L^2} \tag{1}$$

where P_T is the summation of active powers generated by the PV arrays 1 through 4.

As all inverters must operate with same apparent power (i.e. $S_T/4$), the reactive power that inverter 1 must supply is

$$Q_1 = \sqrt{\left(\frac{S_T}{4}\right)^2 - P_1^2} \tag{2}$$

Hence, inverters 2 through 4 must supply the remaining apparent power $S_{T_{new}}$ which is the difference of two vectors

S_T and S_i (where $S_i = \sqrt{P_i^2 + Q_i^2}$) as shown in Fig. 2. As a result, inverters 2 through 4 must supply $S_{Tnew}/3$ for equal apparent power sharing. Thus, the reactive power Q_2 , that inverter-2 must supply is

$$Q_2 = \sqrt{\left(\frac{S_{Tnew}}{3}\right)^2 - P_2^2} \tag{3}$$

Similarly, the reactive powers Q_3 and Q_4 , (and hence apparent power, S_3 and S_4) that inverters 3 and 4 must supply are obtained. This procedure helps to reduce the mismatch in the apparent power sharing. However, it is observed that mismatch in the apparent power sharing varies with the order (sequence) in which the reference reactive powers for the inverters are computed.

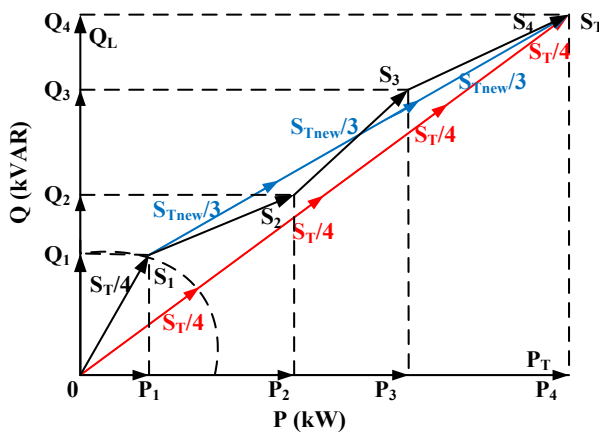


Fig. 2. Reactive power sharing amongst inverters to equalize apparent power of the inverters.

Figure 3 shows the detailed control algorithm for sharing apparent power amongst m identical inverters. It ensures the solution that simultaneously targets two objectives: (i) nearly equal apparent power sharing amongst the inverters and (ii) reduction in the power loss. The principle presented earlier to minimize the mismatch in apparent power of the inverters is implemented in form of sub-routine (referred as ‘Equal S’) shown in Fig. 3(b), while the main program shown in Fig. 3(a) that encases the subroutine, ensures that the equalization of apparent power sharing is achieved without making any compromise with the power losses in the inverters.

The control algorithm shown in Fig. 3(a) evaluates various permutations of scheduling of the inverters which gives the least power loss for the different possible order of allocation. The n permutations of the active powers P_i and nominal apparent power ratings S_{iN} (where $i = 1, 2, 3, \dots, m$) for the m inverters form the $n \times m$ matrices P_{perm} and S_{perm} , respectively. Infact, P_i corresponds to the maximum power P_{MPPi} that i^{th} PV array generates.

For each permutation j , the subroutine computes the available reactive powers Q_i for the inverters ($i = 1, 2, 3, \dots, m$) using corresponding active power $P_{perm}(j, i)$ and apparent power $S_{perm}(j, i)$ as shown through Eqs. (4)-(6). $P_{perm}(j, i)$ and $S_{perm}(j, i)$ are replaced by P_i and S_{iN} respectively, for the sake of simplicity.

$$P_i = P_{perm}(j, i) \tag{4}$$

$$S_{iN} = S_{perm}(j, i) \tag{5}$$

$$Q_i = \sqrt{S_{iN}^2 - P_i^2} \tag{6}$$

The total reactive power support that all the inverters together can provide is

$$Q_T = \sum_{i=1}^m Q_i \tag{7}$$

As the maximum power generated from each PV array must be supplied to the grid, the total power that all the inverters must supply is derived from Eq. (8)

$$P_T = \sum_{i=1}^m P_i \tag{8}$$

Thus, the total apparent power capability of the inverters is expressed by Eq. (9)

$$S_T = \sqrt{P_T^2 + Q_T^2} \tag{9}$$

As it is desired that m inverters must share the apparent power equally, each inverter must provide apparent power S_{new} as computed by Eq. (10)

$$S_{new} = S_T \div [(m + 1) - i] \tag{10}$$

In case $S_{new} > S_{iN}$ indicating i^{th} inverter’s limit is reached, the references S_{new} and Q_{iref} , for apparent and reactive powers are set as S_{iN} and Q_i , respectively.

After assigning the reference active power P_i and reactive power Q_i to the i^{th} inverter, the remaining active and reactive powers to be supplied by the rest of the inverters are updated by subtracting the Q_{iref} and P_i assigned to the earlier inverters. The remaining active power (P_{Tn}) to be supplied and reactive power demand to be met (Q_{Tn}) is calculated using Eqs. (11), and (12), respectively. Apparent power (S_{inew}) that i^{th} inverter must supply can be obtained from P_{Tn} and Q_{Tn} as expressed by Eq. (13).

$$P_{Tn} = P_T - \sum_{i=0}^{i-1} P_i \quad \text{where } P_0 = 0 \tag{11}$$

$$Q_{Tn} = Q_L - \sum_{i=0}^{i-1} Q_{iref} \quad \text{where } Q_{0ref} = 0 \tag{12}$$

$$S_{inew} = \sqrt{P_{Tn}^2 + Q_{Tn}^2} \div ((m + 1) - i) \tag{13}$$

Hence, the reference reactive power for the i^{th} inverter (for j^{th} permutation) is derived as

$$Q_{iref} = \sqrt{S_{inew}^2 - P_i^2} \tag{14}$$

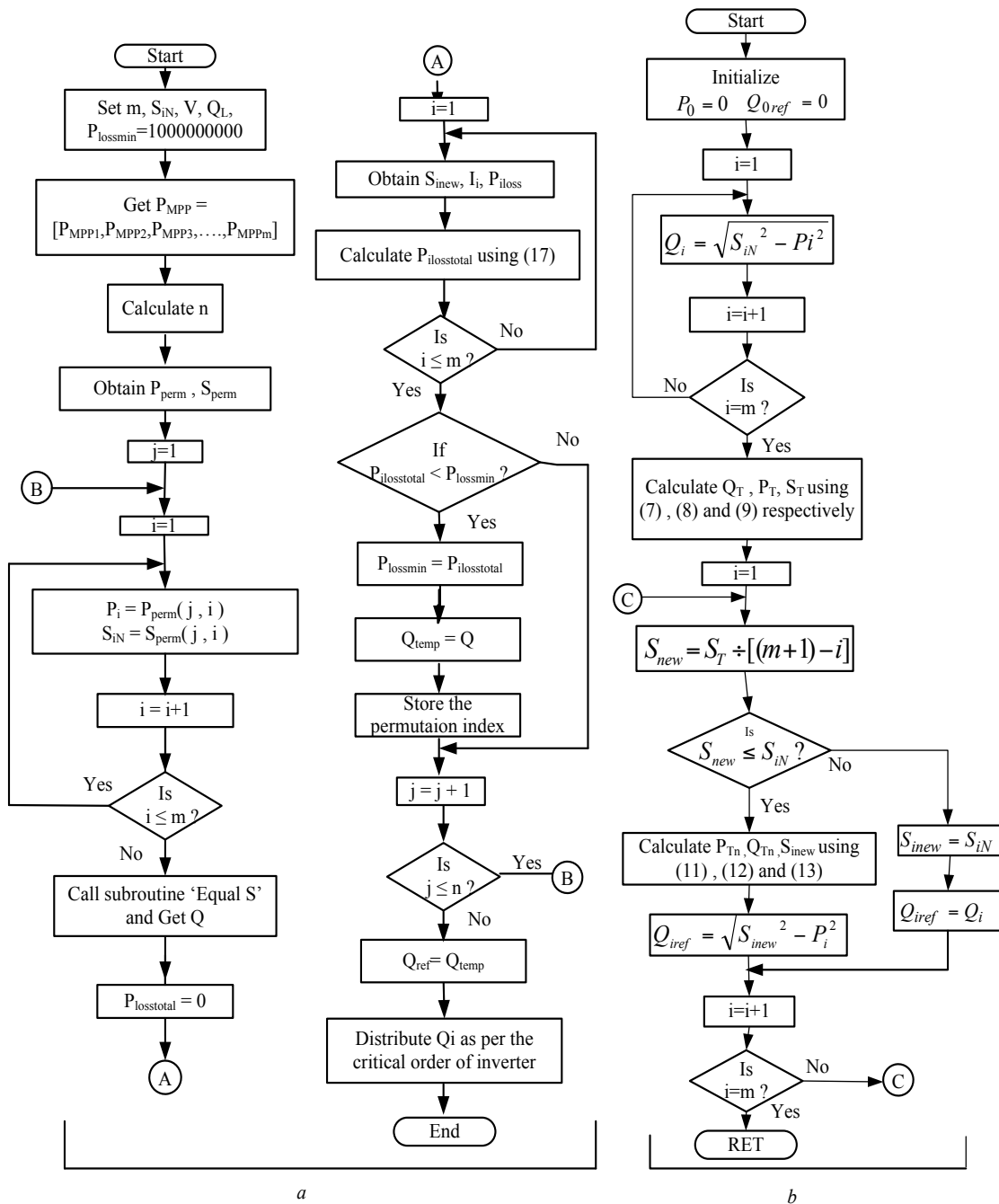


Fig. 3. Flowchart for the proposed EAPS-LL approach (a) Main Program to evaluate the least loss option (b) Subroutine ‘Equal S’ to equalize apparent power

Thus, the matrix Q for j^{th} permutation, that represents the reactive power references for m inverters, is obtained. Finally, the current drawn (I_i) from the i^{th} inverter (for the j^{th}) permutation can be computed as represented by Eq. (15).

$$I_i = \frac{S_{inew}}{\sqrt{3} \times V} \quad (15)$$

where V is line-to-line rms voltage at inverter terminals.

If R represents the equivalent resistance that takes into account the on-state resistance of switches, internal resistance of coupling inductor, transformer etc., power lost in the resistor R for the i^{th} DG can be obtained by Eq. (16).

$$P_{i\text{loss}} = I_i^2 \times R \quad (16)$$

Hence, the total power loss $P_{\text{losstotal}}$, due to the I^2R losses of all m inverters can be represented as

$$P_{\text{losstotal}} = \sum_{i=1}^m P_{i\text{loss}} \quad (17)$$

The process is repeated for all the permutations for $m!$ (m factorial) times to identify the best possible option that gives the least power loss for the system. Initially, the $P_{\text{losstotal}}$ is set to high value ($P_{\text{lossmin}} = 1000000000$) and updated

continuously in process of search of the best option having the least loss. The permutation index for the permutation having the $P_{lossmin}$ is finally used to assign the reference reactive powers Q_{iref} to m inverters in the order 1 through m .

The time required by the algorithm to identify the best possible solution that gives the least losses with relatively good degree of apparent power sharing amongst the DGs is about 0.1s for $m=6$ i.e. five fundamental cycles of 50Hz. The technique can easily be applied for dynamic conditions where the solution from the very first iteration can be set as the reference reactive power for the DGs. The time taken to evaluate the first iteration is much less than even a quarter of a cycle (<0.2ms). The reference (or command) values for reactive power allocation amongst the inverters can then be gradually updated with each iteration if the result of the subsequent iteration is favorable in terms of meeting the objective of least losses.

4. Simulation Results

In order to explore the performance of the system shown in Fig. 1 with the proposed control approach, simulations are done using MATLAB/Simulink. The system parameters adopted for the simulations are summarized in Table 1.

Table 1. Rating and parameters for the system shown in Fig.1.

Parameters	Value
No of PV inverters (m)	6
Nominal power rating of all DGs (S_{IN})	500 KVA
Grid voltage (V_g), Frequency (f)	415 V, 50 Hz
Line parameter (Z_{0i})	L=100μH, R=2.07mΩ, C _f =2500μF
Load	1.16MVA at 0.86 power factor lag
Lumped resistance (R)	0.1Ω

In all cases reported in this section, the system shown in Fig.1 is controlled using four different approaches: ORPS [26], EAPS [29], EAPS-LSD [30] and the proposed EAPS-LL. The performance of the proposed approach EAPS-LL is compared and evaluated with reference to other three approaches (ORPS, EAPS and EAPS-LSD). The performance parameters for comparison are utilization factor of the inverter (UF) and standard deviation for the utilization factors (SD) [27] besides $P_{losstotal}$. Utilization factor is defined as the ratio of apparent power delivered by the inverter to the nominal apparent power rating of the inverter and expressed by Eq. (18) while standard deviation of the utilization factors of the inverters is represented by Eq. (19).

$$UF_i = \frac{S_{inew}}{S_{iN}} \tag{18}$$

$$SD = \sqrt{\frac{1}{(m-1)} \sum_{i=1}^m (UF(i) - UF_{mean})^2} \tag{19}$$

All these approaches perform identically when all the PV arrays operate under identical conditions. Hence, illustrations included here consider only the scenario when the PV arrays generate different amount of power. Reactive power references for inverters are calculated using these algorithms while the active power references are set at the value equal to the maximum power which the corresponding PV system generates at a given instant.

4.1. Case 1: Two different levels of power generation by PV arrays

The case considers that the PV arrays PV₁, PV₂, and PV₃ generate 275kW while the remaining arrays are generating 300kW. The reason for such miss-match can be the shading of some arrays by clouds; some arrays not cleaned and have effect due to soiling; modules of different make for the different groups etc. Reactive power references for these inverters are obtained with different control approaches like ORPS, EAPS, EAPS-LSD and EAPS-LL and are summarized in Tables 2 and 3.

The reactive power references for the inverters with ORPS approach are determined in such a way that the ratio P_i/Q_i for the all the inverters remain the same. Hence, the operating power factor of all the inverters is same. As a result inverters 1 through 3, which are associated with the DGs that generate lesser active power, supply less reactive power. Other three inverters accordingly supply more reactive power to meet the load demand. Hence, the UF of inverters 4,5 and 6 is higher (0.676 as shown in Table 2, 5.5% higher) than that of inverters 1,2 and 3. Unlike ORPS, other three approaches assign the higher reactive power to the inverters carrying lower active power, thereby trying to equalize the apparent power of the inverters. As a result the variation in UF of inverters is insignificant for EAPS, EAPS-LSD and EAPS-LL, indicating uniform heating of the similar components of various DGs for EAPS, EAPS-LSD and EAPS-LL. This is also observed from row corresponding to P_{loss} , which reflects the power loss associated with i^{th} DG. P_{loss} for DGs vary greatly with ORPS while the variation is very less for other three approaches. It is observed that the standard deviation of the utilization factors of the inverters (SD) is higher (0.0301) with ORPS than that obtained with other control approaches (0.0015). The total loss ($P_{losstotal}$) is the least with ORPS (122.34kW) and the highest with EAPS-LSD (122.92kW). However, it can be noticed that the difference in the losses with the different approaches is not that significant.

Fig. 4 shows vector representation of apparent powers shared by the DGs with various control approaches. The vectors S_1 through S_6 for ORPS approach align with each other indicating the operation at same power factor. The operating power factors of each DG and of the system are same. As not much difference in the power sharing is observed for EAPS, EAPS-LSD and EAPS-LL, the vector representations for these approaches show overlap. Unlike ORPS, for the other three control approaches, all the DGs

Table 2. Power sharing with ORPS and EAPS methods for case 1

<i>i</i>	ORPS Method						EAPS Method					
	1	2	3	4	5	6	1	2	3	4	5	6
P_i (kW)	275	275	275	300	300	300	275	275	275	300	300	300
Q_i (kVAR)	144	144	144	156	156	156	172	172	173	128	128	127
S_i (kVA)	310	310	310	338	338	338	324	324	325	326	326	326
UF	0.621	0.621	0.621	0.676	0.676	0.676	0.649	0.649	0.650	0.652	0.652	0.652
P_{loss} (kW)	18.65	18.65	18.65	22.13	22.13	22.13	20.36	20.36	20.43	20.59	20.59	20.54
$P_{loss\ total}$ (kW)	122.34						122.87					
SD	0.0301						0.0015					

Table 3. Power sharing with EAPS-LSD and EAPS-LL methods for case 1

<i>i</i>	EAPS-LSD Method						EAPS-LL Method					
	1	2	3	4	5	6	1	2	3	4	5	6
P_i (kW)	275	275	275	300	300	300	275	275	275	300	300	300
Q_i (kVAR)	173	172	172	128	128	128	172	172	173	128	128	127
S_i (kVA)	325	324	324	326	326	326	324	324	325	326	326	326
UF	0.650	0.649	0.649	0.652	0.652	0.652	0.649	0.649	0.650	0.652	0.652	0.652
P_{loss} (kW)	20.43	20.36	20.36	20.59	20.59	20.59	20.36	20.36	20.43	20.59	20.59	20.54
$P_{loss\ total}$ (kW)	122.92						122.87					
SD	0.0015						0.0015					

operate at different power factors as reflected by the different orientations of vectors S_1 through S_6 . However, the system power factor is still the same as that obtained with ORPS.

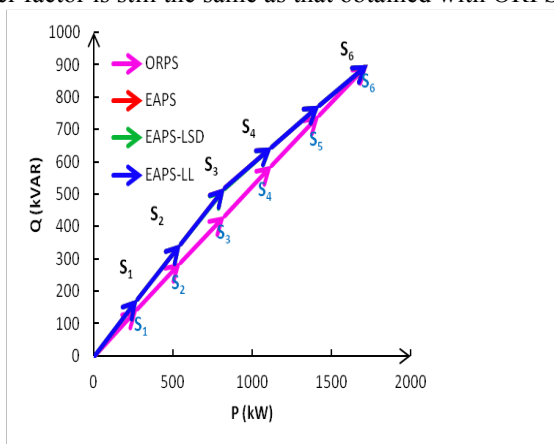


Fig. 4. Vector representation showing power sharing amongst DGs for case 1.

4.2. Case 2: All PV arrays generating different active power

This case explores the performance when the variation in active power generated by different DGs is relatively large. The active power generated by PV arrays PV_1 through PV_6 are 200 kW, 390 kW, 100 kW, 280 kW, 50 kW and 150 kW,

respectively. Tables 4 and 5 present the performance comparisons of the various control approaches in terms of the power shared by the various DGs and the power lost in the DGs. When operating with ORPS approach, inverter-2 supplying the highest active power (390kW), also contributes the maximum to the reactive power requirement (300kVAR). Against it the inverter-4 which supplies the least active power (50kW) provides only 38 kVAR. Thus, inverter-2 operates near its full capacity (98.4%) while inverter-5 operates with UF of 0.126 (12.6%). Consequently, large variations are noticed in the effective utilization of the inverters resulting into $SD=0.3138$. Unlike ORPS, in EAPS inverter 2 and 4 carrying relatively more active power (390 and 280kW, respectively) do not supply any reactive power. Hence, to meet the total reactive power demand other inverters supplying lesser active power have to supply the reactive power, thereby increasing their apparent power. This helps in minimizing the UFs of the inverters and reduces the SD to 0.1088.

In EAPS the reactive power references for the DGs are always calculated in the order 1-2-3-4-5-6. Unlike it, EAPS-LSD identifies the best sequence (out of 720 possible combinations) that gives the least SD for the reactive power allocation. Hence, with EAPS-LSD the SD further reduces to 0.0999 showing better and more uniform utilization of the

Table 4. Power sharing with ORPS and EAPS methods for case 2

<i>i</i>	ORPS Method						EAPS Method					
	1	2	3	4	5	6	1	2	3	4	5	6
P_i (kW)	200	390	100	280	50	150	200	390	100	280	50	150
Q_i (kVAR)	154	300	77	215	38	116	143	0	216	0	284	257
S_i (kVA)	252	492	126	353	63	190	246	390	238	280	288	298
UF	0.505	0.984	0.252	0.706	0.126	0.379	0.492	0.780	0.476	0.560	0.577	0.595
P_{loss} (kW)	12.33	46.86	3.08	24.12	0.76	6.96	11.70	29.44	10.97	15.17	16.09	17.14
$P_{loss\ total}$ (kW)	94.11						100.51					
SD	0.3138						0.1088					

Table 5. Power sharing with EAPS-LSD and EAPS-LL methods for case 2

<i>i</i>	EAPS-LSD Method						EAPS-LL Method					
	1	2	3	4	5	6	1	2	3	4	5	6
P_i (kW)	200	390	100	280	50	150	200	390	100	280	50	150
Q_i (kVAR)	198	40	246	0	248	247	143	0	216	118	237	185
S_i (kVA)	281	392	266	280	253	289	246	390	238	304	242	238
UF	0.563	0.784	0.531	0.560	0.506	0.578	0.492	0.780	0.476	0.608	0.484	0.476
P_{loss} (kW)	15.33	29.75	13.65	15.17	12.39	16.16	11.70	29.44	10.97	17.87	11.35	10.97
$P_{loss\ total}$ (kW)	102.45						92.30					
SD	0.0999						0.1224					

inverters. However, the total power loss increases to 102.45kW as compared to 94.11kW observed with ORPS.

The disadvantage of EAPS-LSD is overcome using EAPS-LL. As observed in Tables 4 and 5, the total loss $P_{loss\ total}$, with EAPS-LL approach is 92.30kW, which is the least when compared to 94.11kW, 100.51kW and 102.45kW resulted with ORPS, EAPS and EAPS-LSD, respectively. The SD for these ORPS, EAPS, EAPS-LSD and EAPS-LL are 0.3138, 0.1088, 0.0999 and 0.1224, respectively. Thus, the power loss with EAPS-LL is 8.89% and 11% lesser, respectively, than that of EAPS and EAPS-LSD approaches with just a marginal increase of 0.022 in SD of UF (compared to EAPS-LSD) of the inverters. EAPS-LL approach first identifies the reactive power references as per principle explained earlier and then evaluates the various order of reactive power allocation to identify the one that gives the least losses rather than the least SD. Hence, EAPS-LL not only minimizes the miss-match in the apparent power of the inverters, but also results into lower power loss ensuring lower and uniform heating of similar components of the various inverters. The power sharing amongst the converters, which is summarized in Tables 4 and 5, is represented in form of vector diagram shown in Fig. 5. It is observed from Fig. 5 that lengths of S_i vectors are more or less equal for EAPS, EAPS_LSD and EAPS-LL approaches while it varies greatly for ORPS method.

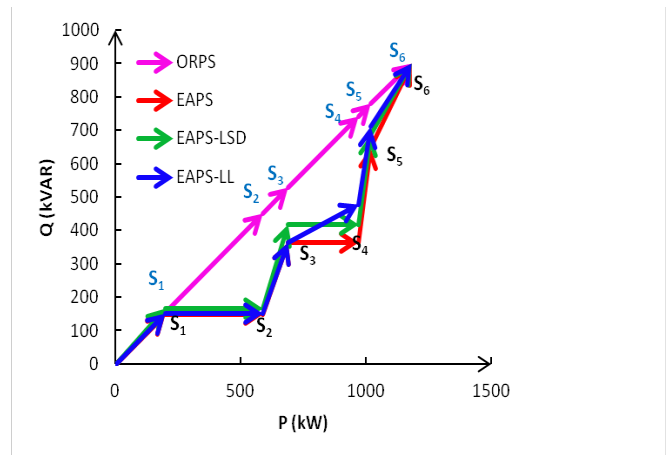


Fig. 5. Vector representation showing power sharing amongst DGs for case 2.

4.3. Case 3: One of the PV array is under maintenance and other generate unequal powers

The performance is also evaluated for the extreme case when one of the PV array (say PV₁) is unable to generate active power due to reasons like scheduled maintenance of PV array, fault on the array of dc-dc converter, total shading, etc. In addition, it is considered that the irradiances on the PV arrays PV₁ through PV₆ are also un-identical. The active power generated by PV arrays PV₁, PV₂, PV₃, PV₄, PV₅ and

PV₆ are 0kW, 50kW, 320kW, 180kW, 100kW and 100kW, respectively. Reactive power references for these inverters are obtained with ORPS, EAPS, EAPS-LSD and EAPS-LL methods and are reported in Tables 6 and 7. It is observed that as PV₁ does not generate active power, with ORPS algorithm its reactive power capability is not utilized. Further, as all the inverters operate at same power factor for ORPS approach, inverter-3 which supplies the highest active power has to contribute the most to the reactive power demand. Hence, the inverter-3 hits its limit i.e. operates with UF=1. Unlike it, for other three approaches inverter-1 also contributes to the reactive power demanded by the load. Further, these methods try to equalize the apparent power of all the inverters. Hence, EAPS, EAPS-LSD and EAPS-LL results into SD equal to 0.0912, 0.0881 and 0.1022, respectively which is about 3.5-4 times less than that obtained with ORPS algorithm. As observed from Table 7, EAPS-LSD results into the least SD. But $P_{loss\ total}$ is relatively higher, about 7.3% higher than that with EAPS-LL approach. Thus, EAPS-LL shows satisfactory operation in terms of realizing nearly equal apparent power sharing without compromising on the efficiency of the system. The power shared by the inverters, which is summarized in Tables 6 and 7, is represented in form of vector diagram shown in Fig. 6. It is observed from Fig. 6 that even for EAPS-LSD and EAPS-LL, all the S_i vectors may not be of nearly equal length. The reason is that for some inverters (here 3), the

active power from the corresponding PV array itself may be too high, even greater than the apparent power of the other inverters. As it is desirable to extract the maximum possible power from each PV array, in some conditions (as with this Case 3) the UFs of the inverters may vary even with EAPS-LSD and EAPS-LL. But the variations are smaller than that obtained with ORPS as depicted by the SD values in Tables 6 and 7 and by lengths of S_i vectors in Fig. 6

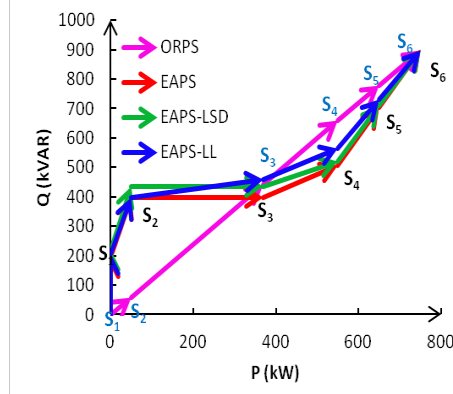


Fig. 6. Vector representation showing power sharing amongst DGs for case 3.

Table 6. Power sharing with ORPS and EAPS methods for case 3

<i>i</i>	ORPS Method						EAPS Method					
	1	2	3	4	5	6	1	2	3	4	5	6
P_i (kW)	0	50	320	180	100	100	0	50	320	180	100	100
Q_i (kVAR)	0	60	384	216	120	120	195	200	0	110	198	198
S_i (kVA)	0	78	500	281	156	156	195	206	320	211	222	222
UF	0	0.156	1	0.562	0.312	0.312	0.390	0.412	0.640	0.422	0.444	0.444
P_{loss} (kW)	0	1.18	48.36	15.3	4.72	4.72	7.36	8.22	19.82	8.61	9.52	9.52
$P_{loss\ total}$ (kW)	74.28						63.05					
SD	0.3523						0.0912					

Table 7. Power sharing with EAPS-LSD and EAPS-LL methods for case 3

<i>i</i>	EAPS-LSD Method						EAPS-LL Method					
	1	2	3	4	5	6	1	2	3	4	5	6
P_i (kW)	0	50	320	180	100	100	0	50	320	180	100	100
Q_i (kVAR)	222	213	0	87	188	190	209	191	60	104	168	168
S_i (kVA)	222	219	320	200	213	215	209	197	326	208	196	196
UF	0.444	0.438	0.640	0.400	0.426	0.429	0.418	0.395	0.651	0.416	0.391	0.391
P_{loss} (kW)	9.54	9.26	19.81	7.73	8.78	8.92	8.45	7.54	20.51	8.36	7.39	7.39
$P_{loss\ total}$ (kW)	64.01						59.64					
SD	0.0881						0.1022					

To illustrate the effectiveness of the dynamic response of the algorithm, a sudden transition from Case 1 to Case 2 is considered at $t=1s$. The active power generated (P_i) for these two cases and the reactive power (Q_i) obtained through the proposed algorithm for the two cases discussed earlier are

Table 8. Active power and Reactive power for Cases 1 and 2

i	Case 1						Case 2					
	1	2	3	4	5	6	1	2	3	4	5	6
P_i (kW)	275	275	275	300	300	300	200	390	100	280	50	150
Q_i (kVAR)	173	172	172	128	128	128	143	0	216	118	237	185
Q_{iact} (kVAR)	189	189	190	140	140	140	154	7	230	126	252	196

It is observed from Fig. 7 that Q_{iact} follows Q_i i.e. have similar nature. However, Q_{iact} is slightly higher than Q_i derived from the proposed algorithm. The reason is the reactive power demanded by the lines (Q_{line}), which is not considered in the calculation. The error could be eliminated if $Q_{load} + Q_{line}$ is used in place of equation Q_{load} in Eq. (1) in the proposed algorithm for calculation of Q_i . The SD of UF has increased just marginally by 0.002 in Case 1 while by 0.009 for Case 2. Thus, the algorithm can effectively perform even in the dynamic conditions.

reproduced again in the Table 8 for the convenience. The reactive powers derived from algorithm, which are set as the references for the inverters are shown in Fig. 7(a) while Fig. 7(b) shows the actual reactive power (Q_{iact}) supplied by the inverters.

operate simultaneously, the active power and the reactive power must be supplied by the inverters in such a way that the PV array and the inverters are optimally utilized. Further, it must be ensured that the inverters must operate below their limits.

The proposed EAPS-LL approach, which is the modification of EAPS-LSD, not only ensures that the inverters (DGs) share the apparent power equally, but also yields a solution that results into lower losses in the inverters. The performance with EAPS-LL is similar to other approaches under uniform insolation conditions when all DGs generate equal active power. However, the results with EAPS-LL approach is the most promising especially when the PV arrays (DGs) generate different active power. With a marginal compromise in the value of SD a significant reduction in the power losses can be achieved with the EAPS-LL approach. Further, the proposed method offers advantages like simplicity, lesser computational burden, no issue of convergence, same number of iterations every time, similar results for each simulation run (as long as there is no change in reactive power demand or variation in the power generation), freedom from issues like initial population selection, non-dominated sorting, diversity preservation etc. over other evolutionary based technique.

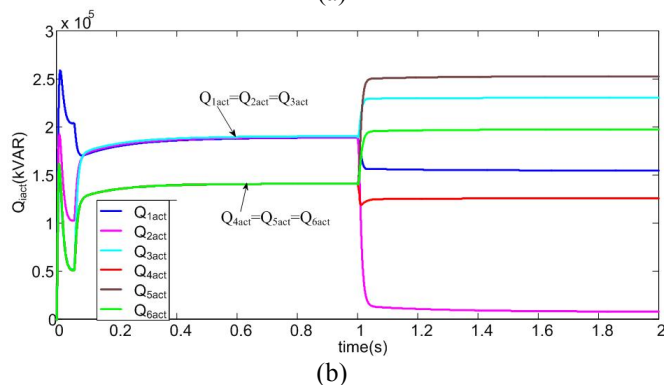
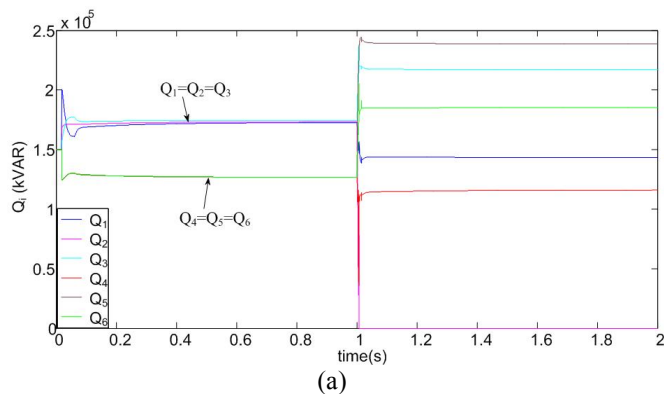


Fig. 7. Reactive power sharing amongst inverters (a) References set by the algorithm (b) Actual reactive power supplied by the inverter.

5. Conclusion

PV based DG is usually intended to generate active power. However, it possesses the capability to provide reactive power compensation. When several such DGs

References

- [1] F. Blaabjerg, R. Teodorescu, M. Liserre, and A. Timbus, "Overview of control and grid synchronization for distributed power generation systems" IEEE Trans. Ind. Electron., vol.53, no.5, pp.1398-1409, October 2006 .
- [2] M. Jazayeri, S. Uysal, and K. Jazayeri K, "A comparative study on different photovoltaic array topologies under partial shading conditions", IEEE PES T&D Conference and Exposition , pp.1-5, 14-17 April 2014.
- [3] M. Ngan and C. Tan, " A study of Maximum Power Point Tracking Algorithms for Stand – alone Photovoltaic Systems". IEEE Applied Power Electronics Colloquium, pp.22-27, 18-19 April 2011.
- [4] X. Li, H. Wen and Y. Hu, "Evaluation of different maximum power point tracking (MPPT) techniques

- based on practical meteorological data", IEEE International Conference on Renewable Energy Research and Applications (ICRERA), pp. 696-701, 20-23 November 2016.
- [5] A. Belkaid, I. Colak and I. Kayisil, "A comprehensive study of different photovoltaic peak power tracking methods", IEEE International Conference on Renewable Energy Research and Applications (ICRERA), pp. 1073-1079, 05-08 November 2017.
- [6] H. Patel, and V. Agarwal, "Maximum power point tracking system for systems operating under partially shaded condition", IEEE Transl. Ind. Electron. , vol.55, no.4, pp.1689–1698, April 2008.
- [7] Z. Salam, J. Ahmed and B. Merugu, "The application of soft computing methods for MPPT of PV system: A technological and status review". Applied Energy, vol.107, pp.135-148, 2013.
- [8] M. Smida, and A. Sakly, "A comparative study of different MPPT methods for grid-connected partially shaded photovoltaic systems". International journal of renewable energy research, vol.6, no.3 pp.1082-1090, 2016.
- [9] A. Dolara, S. Leva, G. Magrati, M. Mussetta, E. Ogliari and R. Arvind "A novel MPPT algorithm for photovoltaic systems under dynamic partial shading — Recurrent scan and track method" IEEE International Conference on Renewable Energy Research and Application, (ICRERA), pp.1122-1127, 20-23 November 2016.
- [10] Y. Hu, J. Zhang, P. Li, D. Yu, and L. Jiang, "Non-uniform aged modules reconfiguration for large scale PV array", IEEE Trans. Device Mater. Rel., vol.17, no.3, pp.560-569, September 2017.
- [11] N. Femia, G. Lisi, G. Petrone, G. Spagnuolo, and M. Vitelli, "Distributed maximum power point tracking of photovoltaic arrays : novel approach and system analysis", IEEE Trans. Ind. Electron., vol.55, no.7, pp.2610-2621, June 2008.
- [12] G. Graditi, G. Adinolfi, and A. Del Giudice, "Experimental performances of a DMPPT multitopology converter", IEEE International Conference on Renewable Energy Research and Applications (ICRERA), pp. 1005-1009, 1005-1009 November 2015.
- [13] E. Dall'Anese, H. Zhu, and G. Giannakis, "Distributed optimal power flow for smart microgrids", IEEE Trans. Smart Grid, vol.4, no.3, pp.1464–1475, September 2013.
- [14] W. Sheng, K. Liu, and S. Cheng, "Optimal power flow algorithm and analysis in distribution system considering distributed generation", IET Gener. Trans. Distrib, vol.8, no.2, pp.261–272, February 2014.
- [15] M. Farasat, and A. Arabali, "Voltage and power control for minimizing converter and distribution losses in autonomous microgrids", IET Gener. Trans. Distrib, vol.9, no.3, pp.1614-1620, September 2015.
- [16] A. Ellis, R. Nelson, E. Engeln, R. Walling, J. McDowell, L. Casey, E. Seymour, W. Peter, C. Barker and B. Kirby, "Reactive power interconnection requirements for PV and wind plants- recommendations to NERC", Report of SANDIA, February 2012.
- [17] Y. Han, H. Li, P. Shen, E. Antônio A. Coelho and J. Guerrero, "Review of active and reactive power sharing strategies in hierarchical controlled microgrids," IEEE Trans. Power Electron., vol. 32, no. 3, pp. 2427–2451, Mar. 2017.
- [18] J. Vasquez, J. Guerrero, and M. Savaghebi, "Modeling, analysis, and design of stationary-reference-frame droop-controlled parallel three-phase voltage source inverters", IEEE Trans. Ind. Electron., vol.60, no.4, pp.1271–1280, April 2013.
- [19] W. Cao, H. Su, J. Cao, J. Sun and D. Yang "Improved droop control method in microgrid and its small signal stability analysis," IEEE International Conference on Renewable Energy Research and Application (ICRERA), pp.197-203, 19-22 October 2014.
- [20] S. Adhikari S, and F. Li, "Coordinated V-f and P-Q control of solar photovoltaic generators with MPPT and battery storage in microgrids", IEEE Trans. Smart Grid, vol.5, no.3, pp.1270-1281, May 2014.
- [21] A. Milczarek, M. Apap, C. Staines and J. Guerrero, "Secondary control for reactive power sharing and voltage amplitude restoration in droop-controlled islanded microgrids" 3rd IEEE International Symposium on Power Electronics for Distributed Generation Systems (PEDG), 25-28 June 2012.
- [22] A. Micallef, M. Apap and J. Guerrero, "Reactive power sharing and voltage harmonic distortion compensation of droop controlled single phase islanded microgrids", IEEE Trans. Smart grid, vol. 5, no. 3, pp. 1149-1158, 2014.
- [23] L. Jingang, L. Xiaoqing, L. Xin, and T. Ruo-Li, "Distributed multiagent-oriented average control for voltage restoration and reactive power sharing of autonomous microgrids", IEEE Access, vol.6, pp. 25551 – 25561, April 2018.
- [24] J. Yanga, W. Yuana, Y. Suna, "A novel quasi-master-slave control frame for PV-storage independent microgrid", Elsevier journal of Electrical Power and Energy Systems, vol. 97, pp. 262-274, 2018.
- [25] P. Sreekumar, V. Khadkikar, "Adaptive power management strategy for effective volt-ampere utilization of a photovoltaic generation unit in standalone microgrids", IEEE Trans. on Ind. Appl., vol. 54, no.2 pp. 1784-1792, 2018.
- [26] Z. Wang, K. Passino, and J. Wang, "Optimal reactive power allocation in large scale grid connected photovoltaic system". Journal of optimization theory and application, Springer, vol.167, no.2, pp.761-779, November 2015.
- [27] Q. Zhong, "Robust droop controller for accurate proportional load sharing among inverters operated in parallel", IEEE Trans. Ind. Electron., vol.60, no.4, pp.1281–1290, April 2013.
- [28] Y. Zhu, F. Zhuo, F. Wang, B. Liu, R. Gou, and Y. Zhao, "A virtual impedance optimization method for reactive power sharing in networked microgrid", IEEE Trans. Ind. Electron., vol.31, no.4, pp.2890-2904, April 2016.
- [29] U. Patel, and H. Patel, "An effective power management strategy for photovoltaic based distributed generation", IEEE International Conference on

Environment and Electrical Engineering (EEEIC), pp.1-6, 7-10 June 2016.

- [30] U. Patel, N. Shah, and H. Patel, "Reactive power management strategy for photovoltaic based distributed generators operating under non- uniform conditions", IEEE International Conference on Power Energy, Environment and Intelligent Control (PEEIC), 12-13 January 2018.